J. Phycol. *, ***–*** (2021)

DOI: 10.1111/jpy.13190

REPRODUCTIVE PHENOLOGY AND MORPHOLOGY OF *MACROCYSTIS PYRIFERA* (LAMINARIALES, OCHROPHYTA) FROM SOUTHERN NEW ZEALAND IN RELATION TO WAVE EXPOSURE[1]

Pablo P. Leal[2]

Department of Botany, University of Otago, 479 Great King Street, Dunedin 9016, New Zealand
Departamento de Repoblación y Cultivo, Instituto de Fomento Pesquero (IFOP), Balmaceda 252, Casilla 665, Puerto Montt, Chile

Michael Y. Roleda

Department of Botany, University of Otago, 479 Great King Street, Dunedin 9016, New Zealand
Norwegian Institute of Bioeconomy Research, Kudalsveien 6, Bodø 8027, Norway
The Marine Science Institute, College of Science, University of the Philippines Diliman, Quezon City, Philippines

Pamela A. Fernández

Centro i mar & CeBiB, Universidad de Los Lagos, Camino a Chinquihue Km 6, Casilla 557, Puerto Montt, Chile

Udo Nitschke

Independent researcher, Jahnstraße 6, Vohburg 85088, Germany

and Catriona L. Hurd

Department of Botany, University of Otago, 479 Great King Street, Dunedin 9016, New Zealand
Institute for Marine and Antarctic Studies, University of Tasmania, 20 Castray Esplanade Battery Point, Hobart, Tasmania 7004, Australia

***Macrocystis pyrifera* is a major habitat forming kelp in coastal ecosystems of temperate regions of the northern and southern hemispheres. We investigated the seasonal occurrence of adult sporophytes, morphological characteristics, and reproductive phenology at two sites within a wave-protected harbour and two wave-exposed sites in southern New Zealand every 3–4 months between 2012 and 2013. Seasonality in reproduction was assessed via the number of sporophylls, the occurrence of sori on sporophylls, and non-sporophyllous laminae (fertile pneumatocyst-bearing blades and fertile apical scimitars), meiospore release, and germination. We found that *M. pyrifera* was present and reproductive year-round in three of the four sites, and patterns were similar for the wave-exposure conditions. Sori were found on pneumatocyst-bearing blades and apical scimitars in addition to the sporophylls, and viable meiospores were released from all three types of laminae. Morphological variations between sites with different wave exposure indicate that sporophytes from wave-protected sites have bigger blades and holdfasts and are longer than those from wave-exposed sites. We discuss the implications of these biological variables for the ecology of *M. pyrifera* inhabiting different wave exposure environments in southern New Zealand.**

Key index words: **hydrodynamics; population dynamic; seasonality; sorus ripeness; sporogenesis; water motion**

***Abbreviations*: MLR, multivariate linear regression**

The subtidal and intertidal rocky shores of most temperate regions are dominated by large kelps that belong to the Order Laminariales (Steneck et al. 2002, Graham et al. 2007a, Flores-Moya 2012, Jayathilake and Costello 2020, 2021). Among them, the forests formed by *Macrocystis pyrifera*, support productive and diverse ecological communities by providing habitat for a wide variety of biota such as marine mammals, fishes, molluscs, and other algae (Mann 1973, Dayton 1985, Steneck et al. 2002, Schiel and Foster 2015, Miller et al. 2018). The global distribution of *M. pyrifera* covers the Pacific coast of North and South America, South Africa, Australasia, and sub-Antarctic islands (Barrales and Lobban 1975, Womersley 1987, van Tussenbroek 1989, Hay 1990, Hoffmann and Santelices 1997, Schiel and Foster 2006, Graham et al. 2007b, Mora-Soto et al. 2020).

Macrocystis pyrifera is a perennial kelp with phenological patterns that are strongly controlled by local environmental conditions, particularly wave action

[1]Received 16 November 2020. Accepted 10 June 2021.
[2]Author for correspondence: e-mail pablo.leal@ifop.cl.
Editorial Responsibility: A. Buschmann (Associate Editor)

(Graham et al. 2007b). Populations of this kelp have striking differences in reproductive strategies depending on local conditions, in both northern and southern hemispheres (Reed et al. 1996, Buschmann et al. 2004, 2006). In the northern hemisphere, in California, *M. pyrifera* has a stable population that reproduces throughout the year, independent of wave exposure (Reed et al. 1996). Similarly, in the southern hemisphere, in northern Chile, in both wave-protected and wave-exposed locations, a stable population of *M. pyrifera* is observed, but with a clearly seasonal reproductive pattern in winter. In contrast, in southern Chile, *M. pyrifera* in wave-exposed populations has stable dynamics, with continuous reproduction similar to California; but in wave-protected sites it has an annual pattern of abundance with sporophytes being present during late winter to summer, but absent in autumn-early winter, and a reproductive season restricted to summer (Buschmann et al. 2004, 2006). The difference between northern and southern Chilean populations has been related to seasonal conditions: *M. pyrifera* from northern locations requires winter conditions (e.g., lower temperatures to trigger reproduction) whereas, in southern locations, *M. pyrifera* is subjected to temperatures appropriate for reproduction throughout the year, which allows them to produce meiospores continuously (Buschmann et al. 2004). Moreover, populations in northern Chile are subjected to less intense storms that allow them to be perennial compared to populations from southern Chile (Buschmann et al. 2004).

Kelps display variable morphologies in response to hydrodynamic conditions, to optimize physiological processes and thrive locally (Hurd et al. 1996, Stevens and Hurd 1997, Blanchette et al. 2002, Wernberg and Thomsen 2005, Koehl et al. 2008, Coppin et al. 2020). In wave-protected sites, kelps typically have wide, thin, flat, and undulated blades (Gerard and Mann 1979, Wernberg and Thomsen 2005, Fowler-Walker et al. 2006, Wing et al. 2007, Hurd and Pilditch 2011). The undulated morphology causes blades to 'flap' under slow flows, thereby periodically stripping diffusion boundary layers and increasing dissolved nutrient and carbon acquisition (Koehl et al. 2008). This flapping also may generate light flecks, preventing self-shading, and enhance photosynthetic rates of blades below (Koehl and Alberte 1988, Wing and Patterson 1993, Wing et al. 2007, Koehl et al. 2008, Raven and Hurd 2012). Wave-exposed kelps have narrow and thick blades with a corrugated surface or serrated edges (Gerard and Mann 1979, Wernberg and Thomsen 2005, Fowler-Walker et al. 2006, Wing et al. 2007, Hurd and Pilditch 2011) that lessen drag forces, thereby reducing mechanical tearing of blades and detachment of the holdfast from the substrate (Cheshire and Hallam 1988, Blanchette 1997, Hurd et al. 1997, Andrew and Viejo 1998, Koehl et al. 2008, de Bettignies et al. 2013).

The growth and morphology of *Macrocystis pyrifera* has been extensively described over the past 100 years (Brandt 1923, Neushul and Haxo 1963, Lobban 1978, Brostoff 1988). Briefly, a macroscopic sporophyte comprises a holdfast, with multiple stipes, and each stipe has an apical scimitar which produces elongated, corrugated blades with basal pneumatocysts. Specialized reproductive laminae, called sporophylls, grow and divide dichotomously above the holdfast. On their surface, sporophylls form sori which is the reproductive tissue that contains haploid biflagellated meiospores (Neushul 1963, Bartsch et al. 2008, Kawai et al. 2013). Upon ripening, meiospores are released to settle, germinate and develop into microscopic male or female gametophytes. After fertilization, the microscopic zygote grows and develops into a new sporophyte (Brandt 1923, Levyns 1933, Papenfuss 1942). The occurrence of sori on non-sporophyllous laminae such as, pneumatocyst-bearing blades and apical scimitars has been reported (Brandt 1923, Neushul 1963, Lobban 1978, Graham et al. 2007b, Leal et al. 2014), where meiospores produced were equally viable compared to those produced by the sporophylls (Leal et al. 2014).

In New Zealand, *Macrocystis pyrifera* grows from Fiordland in the southwest of South Island to Castle Point in south-east of North Island and in Campbell and Auckland Islands (Fig. 1). This kelp forms extensive fringing beds in shallow waters (2–10 m depth) in open coasts and protected harbours where temperatures are <18°C and sufficient nutrients (N and P) are present (Hay 1990). To date, studies on New Zealand's *M. pyrifera* population include its biogeography (Hay 1990, Chin et al. 1991, Pirker 2002), sporophyte morphology and growth (Moore 1942, Kain 1982, Nyman et al. 1990, 1993, Brown et al. 1997), physiology of early life history stages (Leal et al. 2014, 2016, 2017a,b, Leal and Roleda 2018) and adults (Fernández et al. 2014, 2015, 2016, 2017), and alginate chemistry (Mckee et al. 1992). To our knowledge, there are no studies on the reproductive phenology and seasonal occurrence of adult sporophytes of *M. pyrifera* from New Zealand.

This study provides data on the reproductive phenology of *Macrocystis pyrifera* from two sites within a wave-protected harbour and two wave- exposed sites in Otago, southern New Zealand. We hypothesized that the reproductive pattern of *M. pyrifera* from southern New Zealand will be different between wave-exposure conditions, similar to the findings reported for *M. pyrifera* from southern Chile (Buschmann et al. 2004, 2006). To monitor seasonality in reproduction, sporophytes from each site were harvested and a range of parameters were measured: the number of sporophylls, occurrence of sori in sporophylls and non-sporophyllous laminae (i.e., fertile pneumatocyst-bearing blades and fertile apical scimitars), meiospore release and germination, and

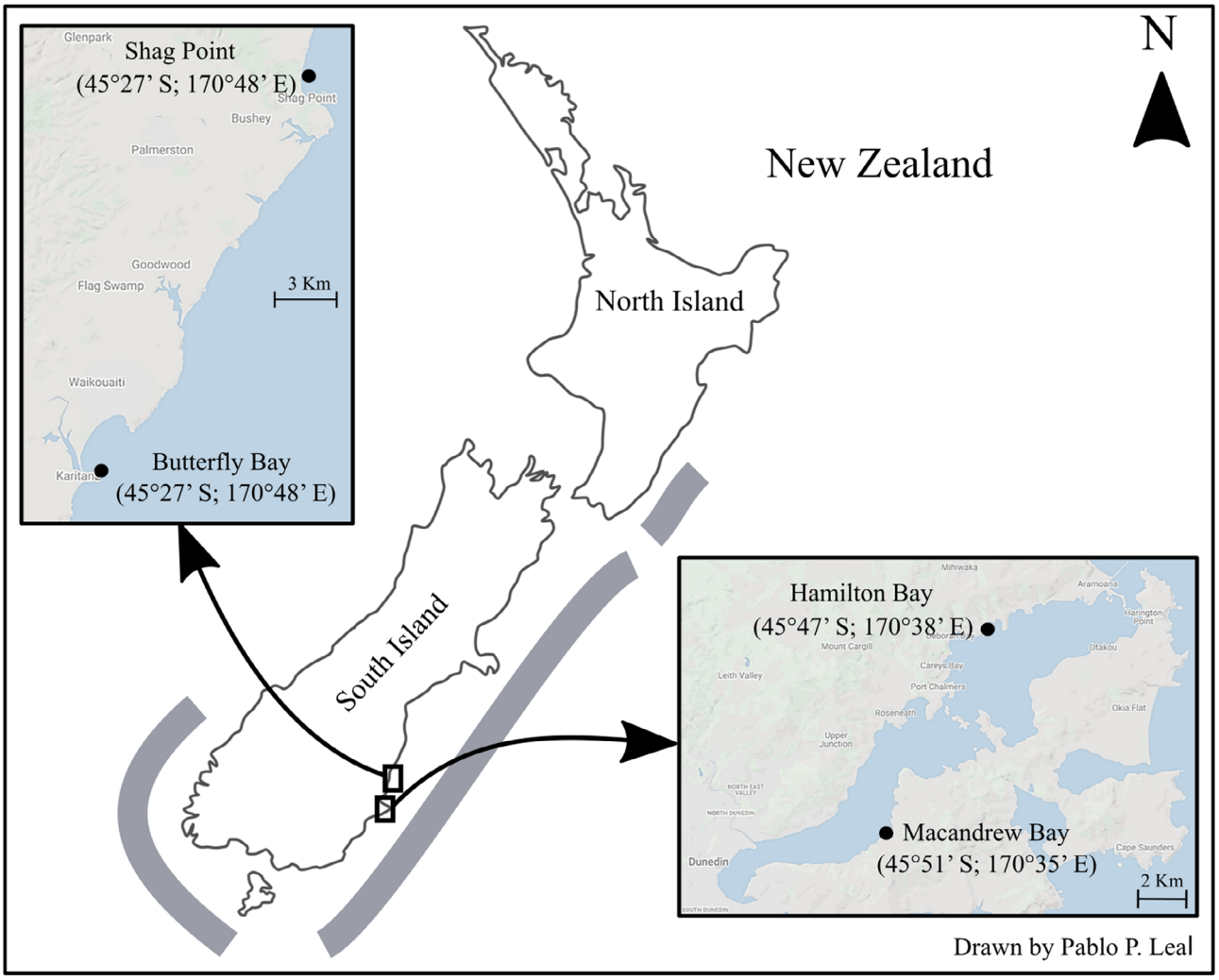

FIG. 1. Study sites in New Zealand's South Island. Butterfly Bay and Shag Point are both exposed to the Pacific Ocean, while Hamilton Bay and Macandrew Bay are inside the Otago Harbour. Gray lines indicate *Macrocystis pyrifera* distribution around the main islands of New Zealand. Modified from Hay (1990).

morphological variability in the adult sporophyte. This new information allows comparison with population dynamics from different biogeographic regions and habitats within those regions. Such knowledge is becoming increasingly critical as the abundance of kelp forests worldwide is declining and under threat by local and global stressors (Johnson et al. 2011, Krumhansl et al. 2016, Filbee-Dexter and Wernberg 2018) and for aquaculture where information about reproduction and seasonality are crucial for kelp cultivation (Camus et al. 2019, Kim et al. 2019).

MATERIAL AND METHODS

Study sites and sample collection. This study was conducted in four sites on the east coast of South Island, New Zealand. The two wave-protected sites were Hamilton Bay (45°47′ S; 170°38′ E) and Macandrew Bay (45°51′ S; 170°35′ E) that are located inside Otago Harbour, sheltered from direct exposure to wind-induced waves and swells. The two wave-exposed sites were Butterfly Bay (45°38′ S; 170°40′ E) and Shag Point (45°27′ S; 170°48′ E), directly exposed to waves and swell in the windy Southern Ocean (Fig. 1). The mean wave high reported for the Otago Harbour ranged between 1.5 and 2 m while in the North Otago Region, it was between 2 and >5 m (Hodgson 1966, Pickrill and Mitchell 1979, Single et al. 2010). At the study sites, *Macrocystis pyrifera* forms shallow and extensive populations at 2–3 m depth in wave-protected sites and 2–6 m depth in wave-exposed sites (GPS Nautical Charts 2020). Sampling was carried out between November (Spring) 2012 and November 2013, when ten entire adult sporophytes were randomly collected in the upper sublittoral of each site during low tide at 1–2 m depth (Table S1 in the Supporting Information).

Fertile laminae and tissue ripeness stages. Fertile structures were classified according to the presence of sori on different types of laminae (Fig. 2). These were sporophylls, which are specialized smooth lamina that grow just above the holdfast and do not have a pneumatocyst; fertile pneumatocyst-bearing blades (hereafter 'fertile blades') that have corrugated surface and grow on the stipes; and fertile apical

scimitars (hereafter 'fertile scimitars') that are lamina with unilateral divisions (Leal et al. 2014).

From each collected sporophyte, fertile and non-fertile sporophylls, and fertile non-sporophyllous laminae (when they were found) were separated, counted and photographed (Table S2 in the Supporting Information). The sorus ripeness was visually qualified into four different stages according to Bartsch et al. (2013): Stage I, vegetative tissue with no visible sorus (uniform light brown appearance); Stage II, pre-mature sorus with slight darkening of fertile tissue; Stage III, mature sorus with dark brown appearance (i.e., with visible sorus); and Stage IV, empty sorus with tissue necrosis and marbled appearance after spore release. The presence of each ripeness stage on the surface of the photographed sporophylls, fertile blades, and fertile scimitars were determined and measured using the image-analysis software ImageJ 1.47v and expressed as percentage of the total lamina area.

Meiospore release and germination. Mature sori (Stage III) from fertile sporophylls and fertile non-sporophyllous laminae were used to determine seasonal patterns of meiospore release and germination success. Meiospore release and cultivation were performed according to Leal et al. (2014). Briefly, discs (1–2 cm^2) cut from fertile tissue were dried by wrapping them in moist tissue paper and incubated overnight at 4°C. Meiospore release was performed by rehydrating the fertile tissue (35 ± 2 g) with 0.2 µm–filtered seawater (300 mL) for 15 min in darkness at 12°C. Thereafter, the sori were removed, and the number of meiospores released during the standardized 15-min period was determined using a hemocytometer (0.1 mm depth, bright-line, Marienfeld, Germany) and expressed as the amount of meiospores per unit volume and unit area. For germination experiments and cultivation purposes, meiospore densities were adjusted to 20,000–25,000 cells $\cdot$ mL^{-1} and separately dispensed onto each compartment of the six-well polystyrene tissue culture vessels (Costar 3516, Corning Incorporated, Corning, NY, USA). Meiospores were cultivated in natural 0.2 µm–filtered seawater at 12°C under a 12:12 h light:dark photoperiod of 50 ± 3 µmol photons $\cdot$ $m^{-2} \cdot s^{-1}$ of PAR (cool-white fluorescent, Philips, Eindhoven, the Netherlands). The number of meiospores that germinated was determined after 3 d from photographs (video camera 5.1 M CMOS camera, UCMOS0510KPA) of at least five randomly chosen visual fields using a 10× objective of an inverted microscope (Olympus CK2; Olympus Optical Co., Ltd., Tokyo, Japan). Photographs were viewed using the digital camera software ToupView 3.5 where 350 meiospores were classified and counted to measure germination percentage according to Leal et al. (2014).

Morphological characteristics. From the ten collected sporophytes, different morphological characters were recorded (in situ measurements and from photographs): total

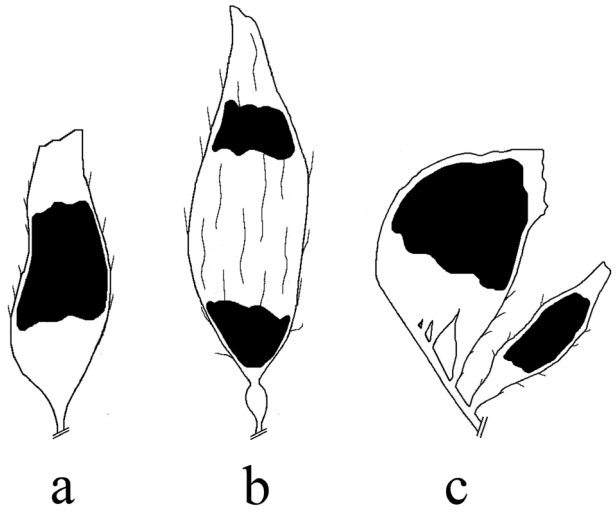

FIG. 2. Sorus-bearing lamina in *Macrocystis pyrifera*. (a) Sporophyll, (b) pneumatocyst-bearing blade, and (c) apical scimitar. Corresponding line illustrations show the typical location where sori (S) are found in each lamina-type. Not drawn to scale. Modified from Leal et al. (2014).

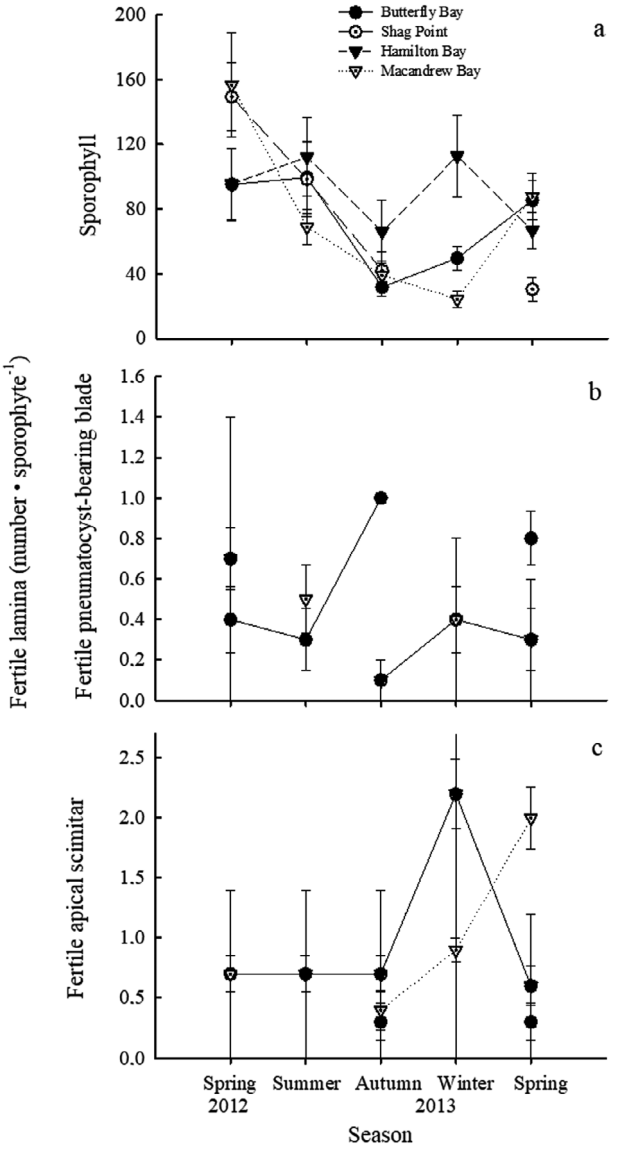

FIG. 3. Annual variation in the number of (a) sporophylls, (b) fertile pneumatocyst-bearing blades and (c) fertile apical scimitars of *Macrocystis pyrifera* from the four study sites (Butterfly Bay, Shag Point, Hamilton Bay, Macandrew Bay). Circles and triangle indicate wave exposure (wave-exposed and wave-protected, respectively), and mean ± SE ($n = 10$). Tukey HSD ($P < 0.05$) showed statistical differences for the number of sporophylls between seasons and fertile pneumatocyst-bearing blades between seasons. Note the different scales in the *y*-axes.

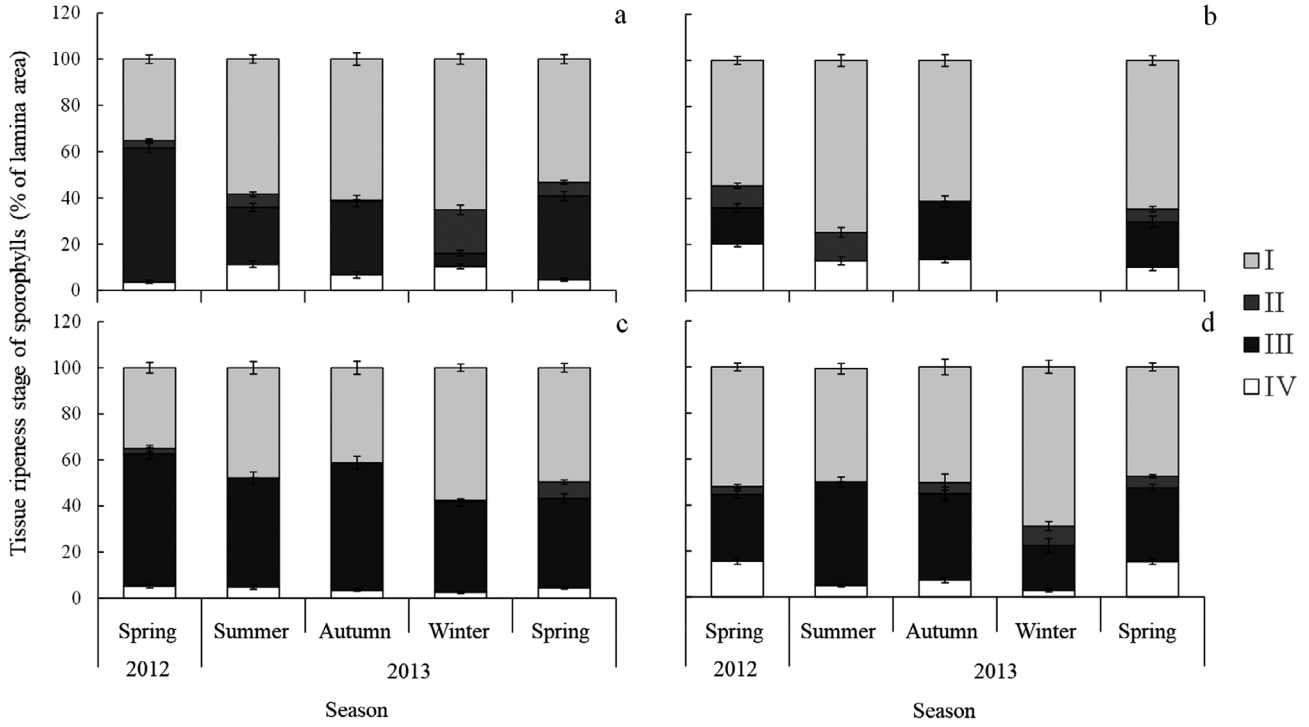

FIG. 4. Annual variation in the tissue ripeness stage (I = vegetative tissue, II = pre-mature sorus, III = mature sorus and IV = empty sorus) of sporophylls of *Macrocystis pyrifera* from (a) Butterfly Bay, (b) Shag Point, (c) Hamilton Bay, and (d) Macandrew Bay. Bars indicate mean ± SE (n can be found in Table S2). Tukey HSD ($P < 0.05$) showed statistical differences for stage I between sites, seasons, and years; for stage III between sites and seasons; and for stage IV between sites and seasons.

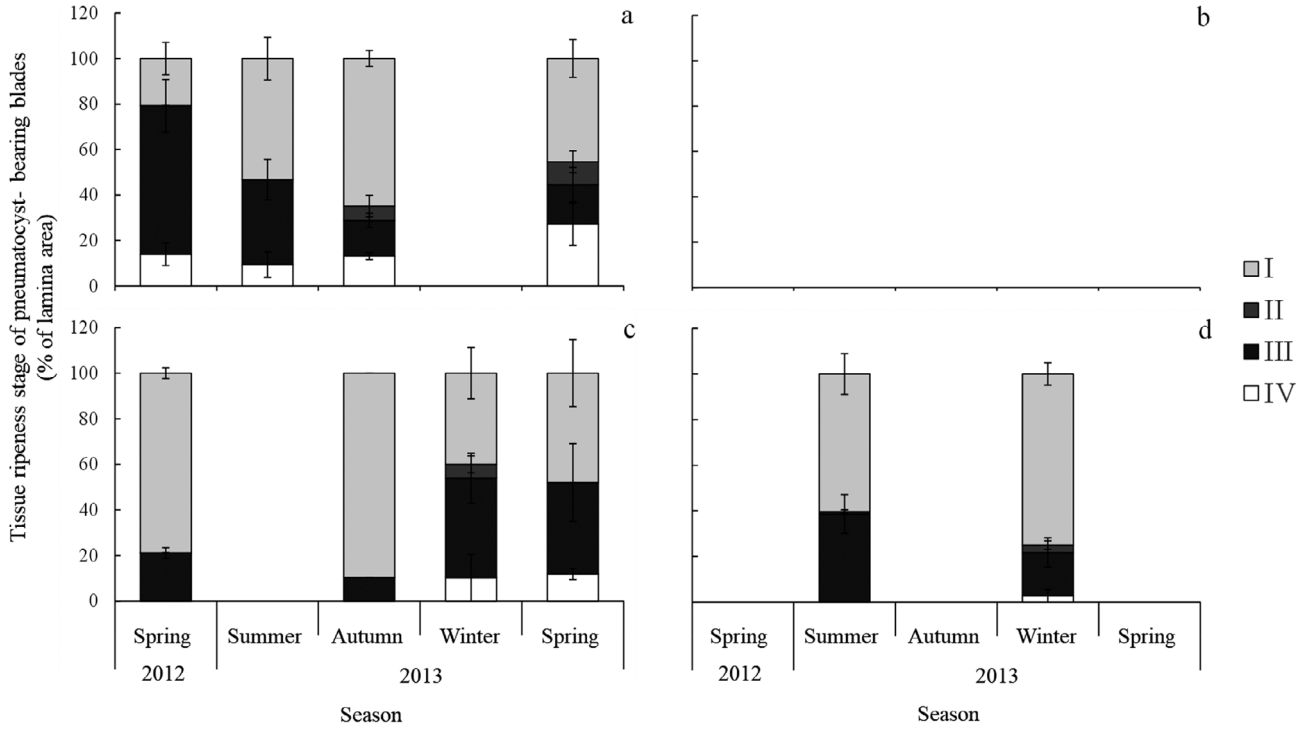

FIG. 5. Annual variation in the tissue ripeness stage (I = vegetative tissue, II = pre-mature sorus, III = mature sorus, and IV = empty sorus) of fertile pneumatocyst-bearing blades of *Macrocystis pyrifera* from (a) Butterfly Bay, (b) Shag Point, (c) Hamilton Bay, and (d) Macandrew Bay. Bars indicate mean ± SE (n can be found in Table S2). Tukey HSD ($P < 0.05$) showed statistical differences for stage IV between years.

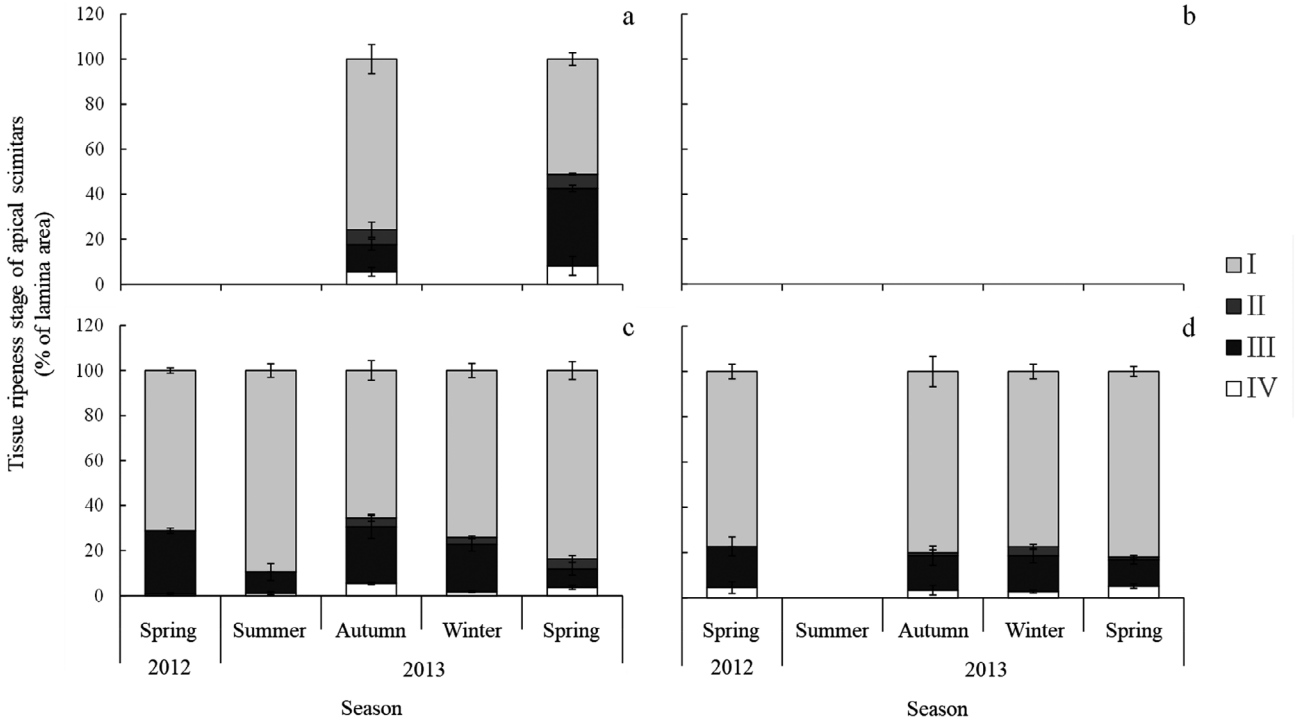

FIG. 6. Annual variation in the tissue ripeness stage (I = vegetative tissue, II = pre-mature sorus, III = mature sorus, and IV = empty sorus) of apical scimitars of *Macrocystis pyrifera* from (a) Butterfly Bay, (b) Shag Point, (c) Hamilton Bay, and (d) Macandrew Bay. Bars indicate mean ± SE (n can be found in Table S2). Tukey HSD ($P < 0.05$) showed statistical differences between seasons for stage I and stage IV.

sporophyte length, the number of stipes produced by each holdfast, holdfast size (length and width), vegetative blade size (length, width and basal angle), and pneumatocyst size (length and width). Holdfast, vegetative blade and pneumatocyst morphology characters were measured from photographs using the image-analysis software ImageJ 1.47v.

Nutrient concentration in seawater. Inorganic nutrient concentrations were measured from 10 mL–filtered seawater samples (0.2 µm, Whatman™ Polycap™ TC filter capsule; GE Healthcare Life Sciences, Buckinghamshire, UK) taken in replicates ($n = 3$) during each sample collection. In the laboratory, seawater samples were frozen at −20°C until analysis for NH_4^+, NO_3^-, and PO_4^{3-} using a QuickChem 8500 series 2 Automated Ion Analyzer (Lachat Instrument, Loveland, CO, USA).

Statistical analysis. A MLR analysis was used to determine effects of the explanatory variables "Site", "Season", and "Year" on the response variables (fertile laminae, ripeness stage, meiospore release and germination, sporophyte length and number of stipes, holdfast length and width, vegetative blade length and width, pneumatocyst length and width, and nutrient concentrations). Response variables were log or arcsine transformed when raw data did not meet the test assumptions. The explanatory variable "exposure" (with two levels: wave-exposed and wave-protected) was dropped from the analysis due to high collinearity with "site". "Site" was included in the analysis because it provided more information than "exposure". Type III sum of squares (SS) were calculated. Tukey HSD tests were applied for multiple pairwise comparisons. Significant effects were quantified by means of partial eta-squared ($p\eta^2$). See Tables S3-S9 in the Supporting Information for details of statistical results for each variable. All statistical analyses were conducted using IBM SPSS Statistics (version 24).

RESULTS

Fertile laminae. Fertile sporophylls were found at Hamilton Bay, Macandrew Bay, and Butterfly Bay in all seasons whereas at Shag Point fertile sporophylls were found in all seasons except winter. The number of sporophylls per sporophyte ranged from 23 to 155 lamina (Fig. 3a) and varied between seasons (MLR: $F_{3,174} = 3.04$, $P = 0.0304$, $p\eta^2 = 0.050$) with the highest number observed in summer and spring (Table S3). Fertile blades and fertile scimitars were found in Hamilton Bay, Macandrew Bay, and Butterfly Bay but not found at Shag Point during any season (Fig. 3; Tables S1 and S2). The number of fertile blades per sporophyte ranged from 0.3 to 1.0 lamina (Fig. 3b) and varied between sites and seasons (MLR: $F_{3,92} = 6.457$, $P = 0.0024$, $p\eta^2 = 0.123$) with the highest number observed in autumn, but without a clear site pattern (Table S7). The number of fertile scimitars per sporophytes ranged between 0.30 and 2.20 lamina (Fig. 3c) and varied between sites and seasons (MLR: $F_{3,100} = 14.153$, $P < 0.0001$, $p\eta^2 = 0.298$) with the highest number observed in winter, but without a clear site pattern (Table S3).

Ripeness stages of fertile tissue. All four stages of sorus ripeness were identified on the surface of the sporophylls and non-sporophyllous laminae. Across all lamina types, the surface area of Stage I ranged from 21 to 90%, Stage II between 0 and 90%, Stage III between 0 and 65%, and Stage IV between 0 and

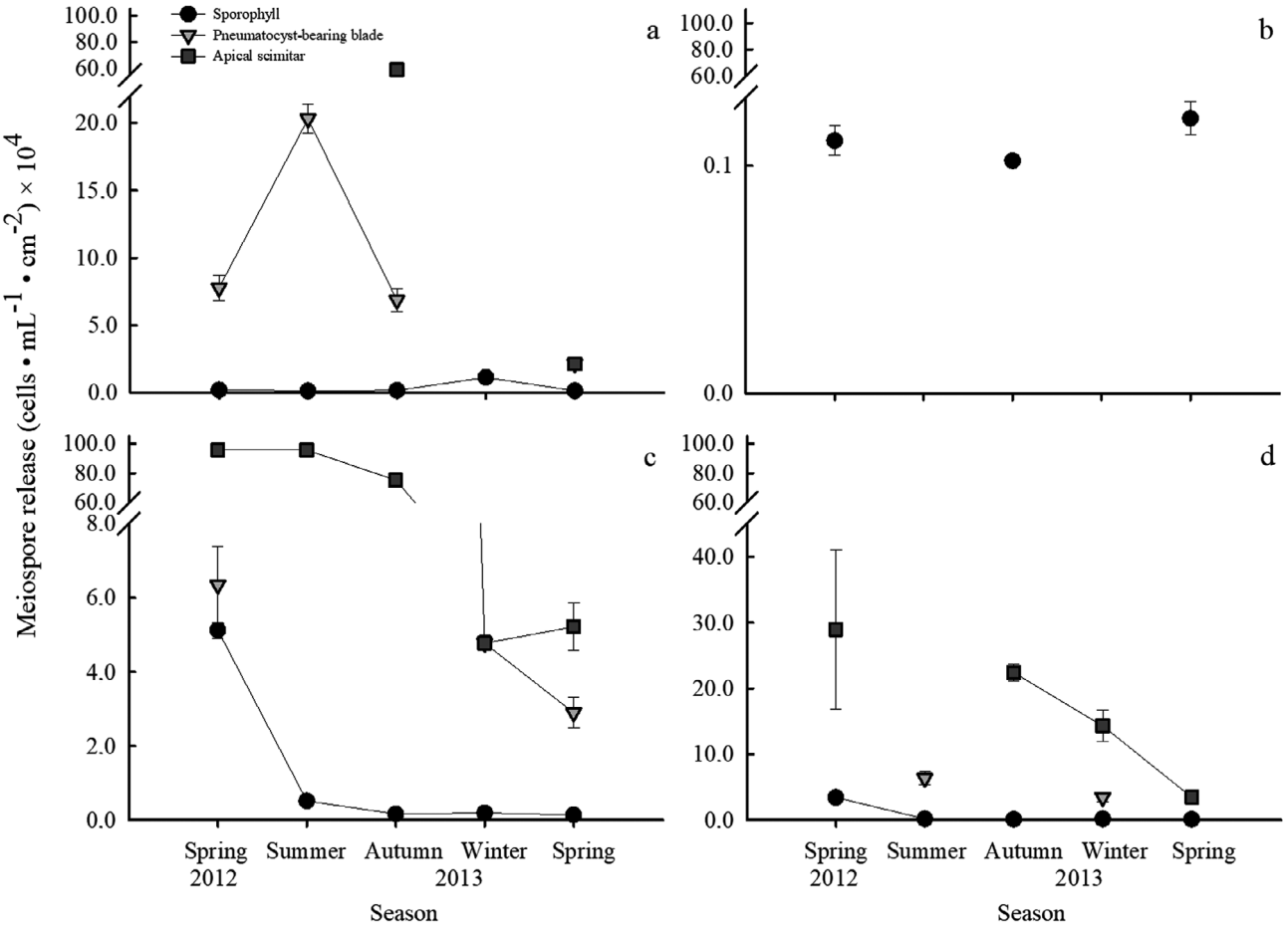

FIG. 7. Annual variation in meiospore release from fertile sporophylls, fertile pneumatocyst-bearing blades, and fertile apical scimitars of *Macrocystis pyrifera* from (a) Butterfly Bay, (b) Shag Point, (c) Hamilton Bay, and (d) Macandrew Bay. Bars indicate mean ± SE ($n = 6$). Tukey HSD ($P < 0.05$) showed statistical differences for meiospore release from sporophylls between sites and seasons, from fertile pneumatocyst-bearing blades between seasons, and from fertile apical scimitars between seasons. Note the break and different scales in the *y*-axes.

27% (Figs. 4–6). Stage III (mature sorus) was observed at all sites and did not show a seasonal pattern. On sporophylls, the surface area of Stage III ranged from 0 to 58% (Fig. 4) and varied between sites and seasons (MLR: $F_{8,173} = 9.795$, $P < 0.0001$, $p\eta^2 = 0.312$) with the highest percentage observed in Hamilton Bay in autumn (Table S4). On fertile blades, Stage III surface area ranged from 10 to 65% (Fig. 5) and did not differ between sites nor seasons (Table S5). On fertile scimitars, Stage III surface area ranged from 8.2 to 34% (Fig. 6) and varied between sites and seasons (MLR: $F_{3,85} = 3.562$, $P = 0.0175$, $p\eta^2 = 0.112$), but without a clear pattern (Table S6).

Meiospore release. Meiospores were released from Stage III-sori of sporophylls and non-sporophyllous lamina in all seasons and at all sites, but there were no seasonal patterns (Fig. 7). Densities of released meiospores from fertile sporophylls during the 15-min period ranged between 0.10×10^4 and 5.13×10^4 cells $\cdot$ mL^{-1} $\cdot$ cm^{-2} (Fig. 7) and varied between sites and seasons (MLR: $F_{1,39} = 37.899$, $P = 0.0002$, $p\eta^2 = 0.492$) with the highest meiospore density observed in those from Shag Point in autumn (Table S7). For the meiospores released by fertile blades during the same 15-min period, densities ranged between 2.13×10^4 and 20.31×10^4 cells $\cdot$ mL^{-1} $\cdot$ cm^{-2} (Fig. 7) and varied between seasons (MLR: $F_{3,19} = 15.641$, $P < 0.0001$, $p\eta^2 = 0.711$) with the highest density occurring on spring (Table S7). Densities of meiospores released by fertile scimitar ranged between 2.13×10^4 and 95.68×10^4 cells $\cdot$ mL^{-1} $\cdot$ cm^{-2} (Fig. 7) and varied between seasons (MLR: $F_{3,23} = 23.783$, $P < 0.0001$, $p\eta^2 = 0.757$) with the highest density occurring in spring (Table S7).

Meiospore germination. After 3 d, germination of meiopores released by sporophylls and non-sporophyllous laminae was not significantly different. Germination of meiospore released from fertile sporophylls ranged from 38 to 86% (Fig. 8) and varied between sites and seasons (MLR: $F_{7,39} = 13.639$,

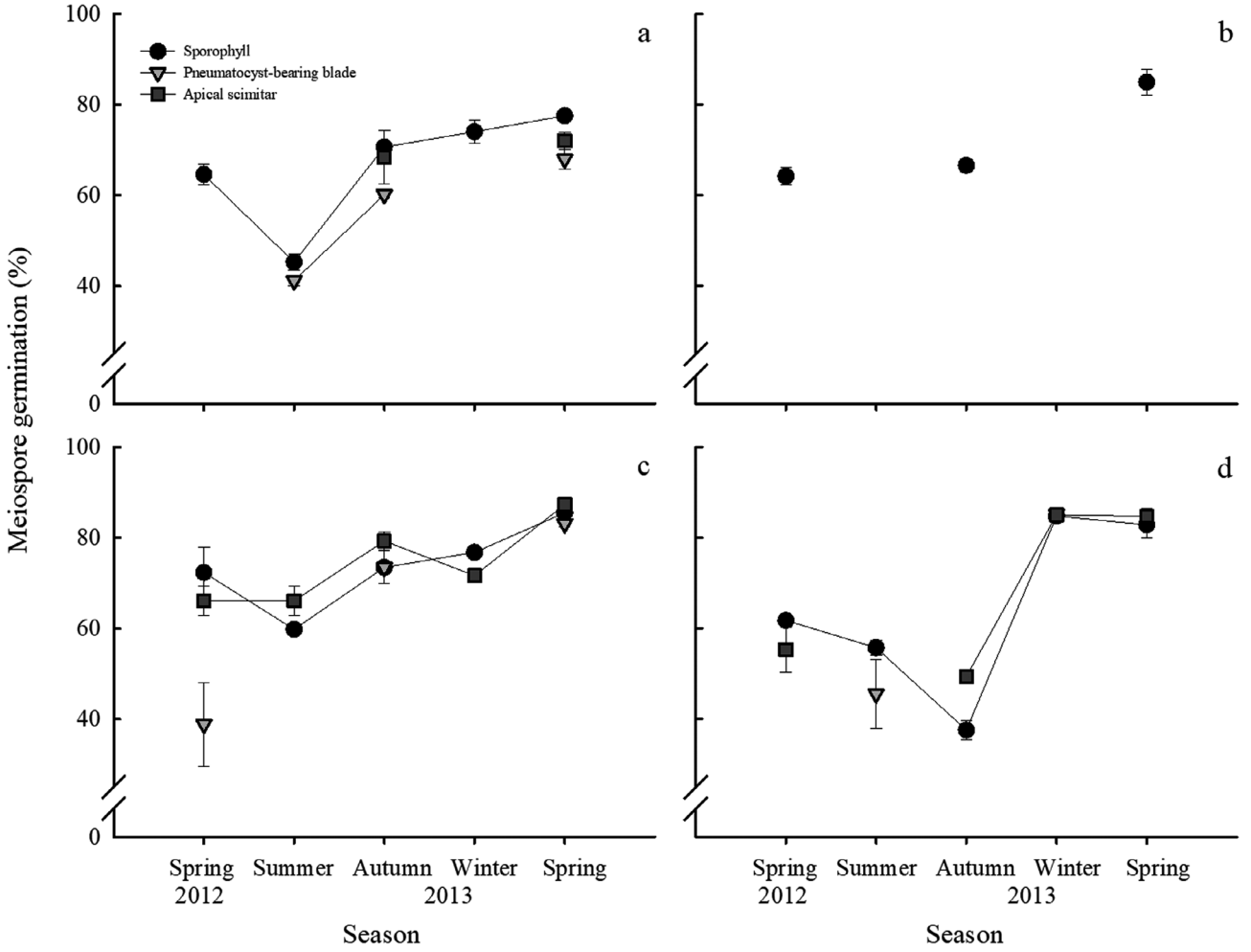

FIG. 8. Annual variation in meiospore germination from fertile sporophylls, fertile pneumatocyst-bearing blades and fertile apical scimitars of *Macrocystis pyrifera* from (a) Butterfly Bay, (b) Shag Point, (c) Hamilton Bay, and (d) Macandrew Bay. Bars indicate mean ± SE ($n = 6$). Tukey HSD ($P < 0.05$) showed statistical differences for meiospore germination from sporophylls between sites and seasons, from fertile pneumatocyst-bearing blades between seasons, and from fertile apical scimitars between seasons. Note the break in the *y*-axes.

$P < 0.0001$, $p\eta^2 = 0.710$) with the highest percent germination observed in those collected from Hamilton Bay and Shag Point in winter and spring (Table S8). Germination of meiospores released by fertile blades ranged from 39 to 85% (Fig. 8) and varied between seasons (MLR: $F_{3,16} = 10.148$, $P = 0.0006$, $p\eta^2 = 0.656$) with the highest percent germination during winter (Table S8). The germination of meiospores released by fertile scimitars ranged from 49 to 87% (Fig. 8) and varied between sites and seasons (MLR: $F_{3,23} = 20.642$, $P < 0.0001$, $p\eta^2 = 0.728$), with the highest percentage during winter and spring, but without a clear site pattern (Table S8).

Morphological characteristics. Morphological characters of adult sporophytes from each site are shown in Figure 9. Sporophytes were found in Macandrew Bay, Hamilton Bay and Butterfly Bay year-round, but were absent in Shag Point during winter (Fig. 10a; Table S1). The length of sporophytes ranged between 1.1 and 5.7 m (Fig. 10a) with the longest observed in Macandrew Bay and Hamilton Bay, varying between sites and seasons (MLR: $F_{8,174} = 4.349$, $P < 0.0001$, $p\eta^2 = 0.167$), but with no clear seasonal pattern (Table S3). The number of stipes per adult sporophyte varied between 1.3 and 4.9 stipes (Fig. 10b) and did not differ between sites and seasons (Table S3). Holdfast length ranged between 12.5 and 32.7 cm (Fig. 11) and varied between sites (MLR: $F_{3,174} = 12.889$, $P < 0.0001$, $p\eta^2 = 0.182$) and seasons (MLR: $F_{3,174} = 6.243$, $P = 0.0005$, $p\eta^2 = 0.097$) with the longest holdfasts observed in Hamilton Bay in summer (Table S3). Holdfast width ranged between 13 and 27 cm (Figure S1 in the Supporting Information) but this variable was removed from the statistical analysis due to high collinearity with the holdfast length.

Vegetative blade morphology. Morphological characteristics of vegetative blades (basal angle, length and

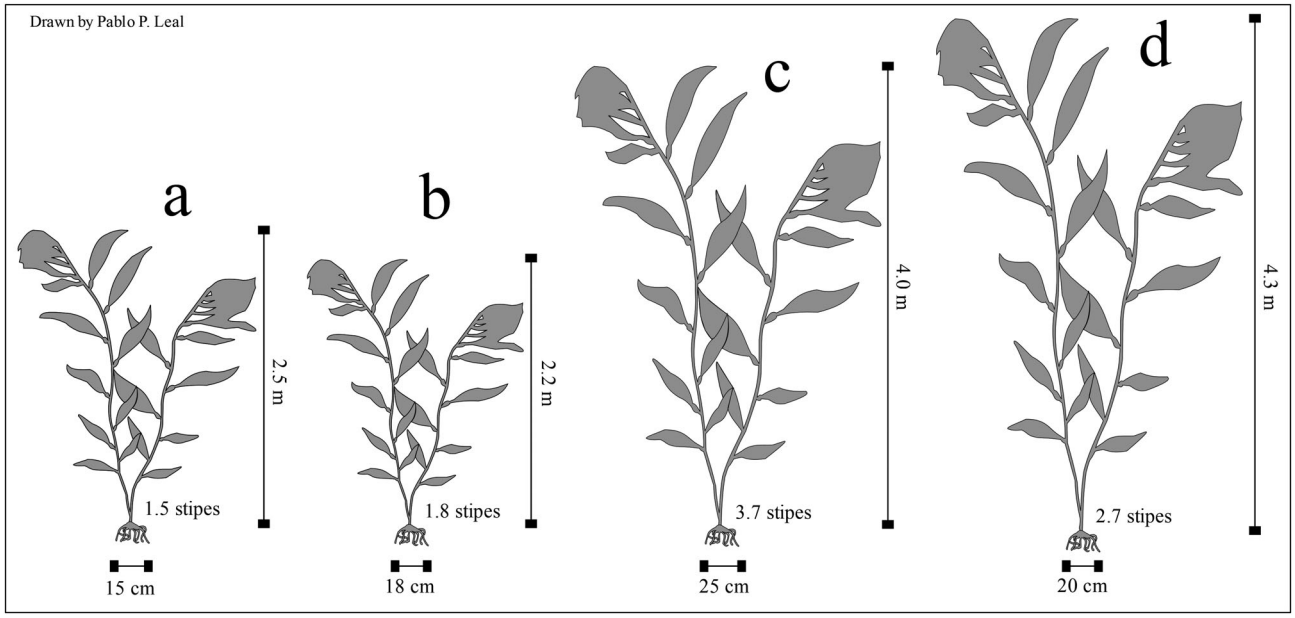

FIG. 9. Variations in average sporophyte length, holdfast width and stipe number of *Macrocystis pyrifera* sporophytes from (a) Butterfly Bay, (b) Shag Point, (c) Hamilton Bay, and (d) Macandrew Bay. See text for details.

width) and pneumatocysts (length and width) are shown in Figure 12. The basal angle of vegetative blades ranged between 64° and 137° (Fig. 13a) and varied between sites and seasons (MLR: $F_{8,174} = 2.985$, $P = 0.0037$, $p\eta^2 = 0.121$) with the widest basal angle observed in Hamilton Bay, Butterfly Bay, and Macandrew Bay in summer (Table S3). Length of vegetative blades ranged between 39 and 93 cm (Fig. 13b) and varied between sites and seasons (MLR: $F_{8,174} = 13.081$, $P < 0.0001$, $p\eta^2 = 0.376$) with the longest vegetative blades observed in Macandrew Bay in winter and spring (Table S3). The width of vegetative blades ranged between 4.6 and 12 cm (Figure S2 in the Supporting Information) but this variable was removed from the statistical analysis due to high collinearity with the vegetative blade length. Length of pneumatocysts ranged between 3.2 and 6.3 cm (Fig. 14) and varied between sites and seasons (MLR: $F_{8,174} = 8.380$, $P < 0.0001$, $p\eta^2 = 0.278$) with the longest pneumatocysts observed in Macandrew Bay (Table S3). Pneumatocyst width ranged between 1.1 and 2 cm (Figure S3 in the Supporting Information) and varied between sites and seasons (MLR: $F_{8,174} = 4.851$, $P < 0.0001$, $p\eta^2 = 0.182$) with the widest pneumatocysts observed in Shag Point and Butterfly Bay, but there was no clear seasonal pattern (Table S3).

Nutrient concentrations. The concentration of NH_4^+, NO_3^-, and PO_4^{3-} in seawater varied significantly between seasons and sites (Table S9). Concentrations of NH_4^+ ranged between 0.51 and 4.38 μM NH_4^+ (Fig. 15a) and differed between sites and seasons (MLR: $F_{9,43} = 2.64$, $P = 0.0158$, $p\eta^2 = 0.356$) with the highest concentrations observed in summer and autumn, although a clear site-specific pattern was not observed (Table S9). For NO_3^-, concentrations ranged between 0.62 and 7.17 μM NO_3^- (Fig. 15b) and differed between sites and seasons (MLR: $F_{9,43} = 2.68$, $P = 0.0145$, $p\eta^2 = 0.360$) with higher concentrations observed in Shag Point and Butterfly Bay in autumn and winter (Table S9). Concentrations of PO_4^{3-} ranged between 0.13 and 1.27 μM PO_4^{3-} (Fig. 15c) and differed between sites and seasons (MLR: $F_{9,43} = 9.537$, $P < 0.0001$, $p\eta^2 = 0.666$) with the highest concentrations observed in summer and autumn, but there was no clear site-specific pattern (Table S9).

DISCUSSION

In three of the four sites, sporophytes of *Macrocystis pyrifera* were present and reproductive year-round, indicating that those populations are perennial. This result is similar to the phenological pattern described for *M. pyrifera* populations from California (Reed et al. 1996) and those from wave-exposed areas in southern Chile (Buschmann et al. 2004, 2006). The exception was the wave-exposed Shag Point where a discontinuous pattern of fertility was observed: sori in the sporophylls did not mature into Stage III in summer, and sporophytes were absent in winter, likely due to their dislodgement as a result of storm surge or seasonally strong wave-exposure. The same was observed in central California where around 50% of *M. pyrifera* canopy was dislodged after winter storm surges (Reed et al. 2008, 2011). Had the adult giant kelp sporophytes not

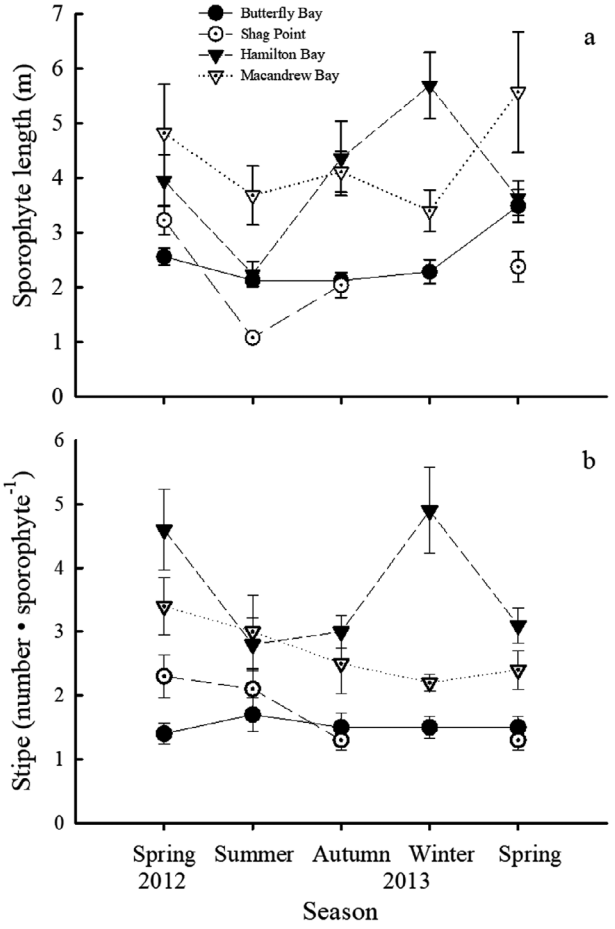

FIG. 10. Annual variation in (a) sporophyte length and (b) number of stipes per sporophyte of *Macrocystis pyrifera* from the four study sites (Butterfly Bay, Shag Point, Hamilton Bay, Macandrew Bay). Circles and triangle indicate wave exposure (wave-exposed and wave-protected, respectively) and mean ± SE ($n = 10$). Note the different scales in the *y*-axes. Tukey HSD ($P < 0.05$) showed statistical differences for sporophyte length between sites.

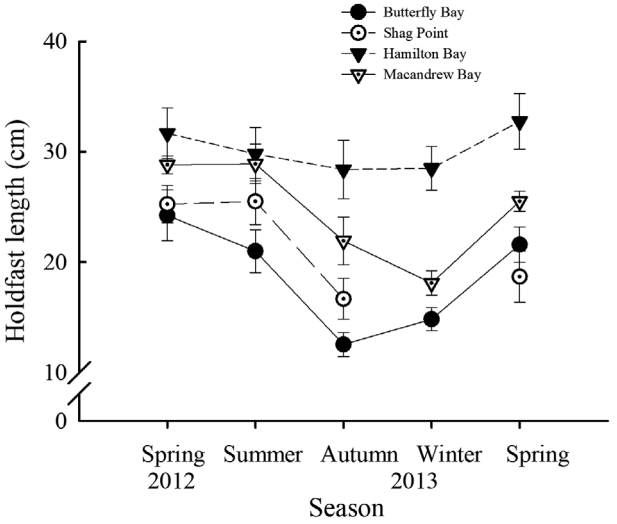

FIG. 11. Annual variation in holdfast length width of *Macrocystis pyrifera* from the four study sites (Butterfly Bay, Shag Point, Hamilton Bay, Macandrew Bay). Circles and triangle indicate wave exposure (wave-exposed and wave-protected, respectively) and mean ± SE ($n = 10$). Tukey HSD ($P < 0.05$) showed statistical differences for holdfast length between sites and season. Note the break and different scales in the *y*-axes.

been lost in Shag Point, they could have been reproductive. At our wave-protected sites, we neither observed a seasonal pattern in adult occurrence nor reproduction; this is comparable to the observation for wave-protected sites in northern and southern Chile (Buschmann et al. 2004, 2006).

In wave-protected sites, we found more fertile non-sporophyllous laminae than in wave-exposed sites. The importance of sorus production on the distal non-sporophyllous lamina for dispersal and recruitment has not been investigated. However, Leal et al. (2014) hypothesized that, in wave-protected sites, sori produced on pneumatocyst-bearing blades and scimitars located in apical blades of the sporophyte may enhance short-distance dispersal during low tide when fronds of *Macrocystis pyrifera* lie prostate and close to the benthos, releasing meiospores some meters away from those released by the basal sporophylls. The reduced number of fertile non-sporophyllous laminae found at wave-exposed sites is likely due to mechanical tearing of the mid to apical portions of the sporophytes. In extreme cases, the whole sporophyte may be dislodged from the substrate during seasonally strong water movement and storm surge (Reed et al. 2008, 2011, Roleda and Dethleff 2011). The removal of apical vegetative tissue from *M. pyrifera* can reduce sporophyll production by 90% (Reed 1987) and stop sporogenesis 9 d after vegetative tissue removal (Graham 2002), indicating that reproduction depends on energy allocation from the upper part of the sporophyte. Considering that reproduction is energetically expensive, allocation of reproductive effort in specialized tissues or basal parts of the thallus that have a lower risk of getting damaged or lost (e.g., basal sporophylls, basal stipe and holdfast; Kawai et al. 2013, Akita et al. 2016, Liu et al. 2017) may be selected to avoid wasting resources when strong wave action breaks away the distal and/or apical parts of the frond that bears fertile blades and/or fertile scimitars. These hypotheses need to be tested to understand the role of producing sori on distal pneumatocyst-bearing blades and scimitars, against localizing reproduction in specialized tissues or other basal parts of the sporophyte.

Individuals of *Macrocystis pyrifera* from Shag Point were absent in winter but present in the following spring. At this site, *M. pyrifera* may have a strategy to ensure a fast recovery after individuals disappear in winter storms, including the release of a high and constant density of meiospores during previous seasons. These meiospores may create a "seed bank" of dormant microscopic stages (Chapman 1987,

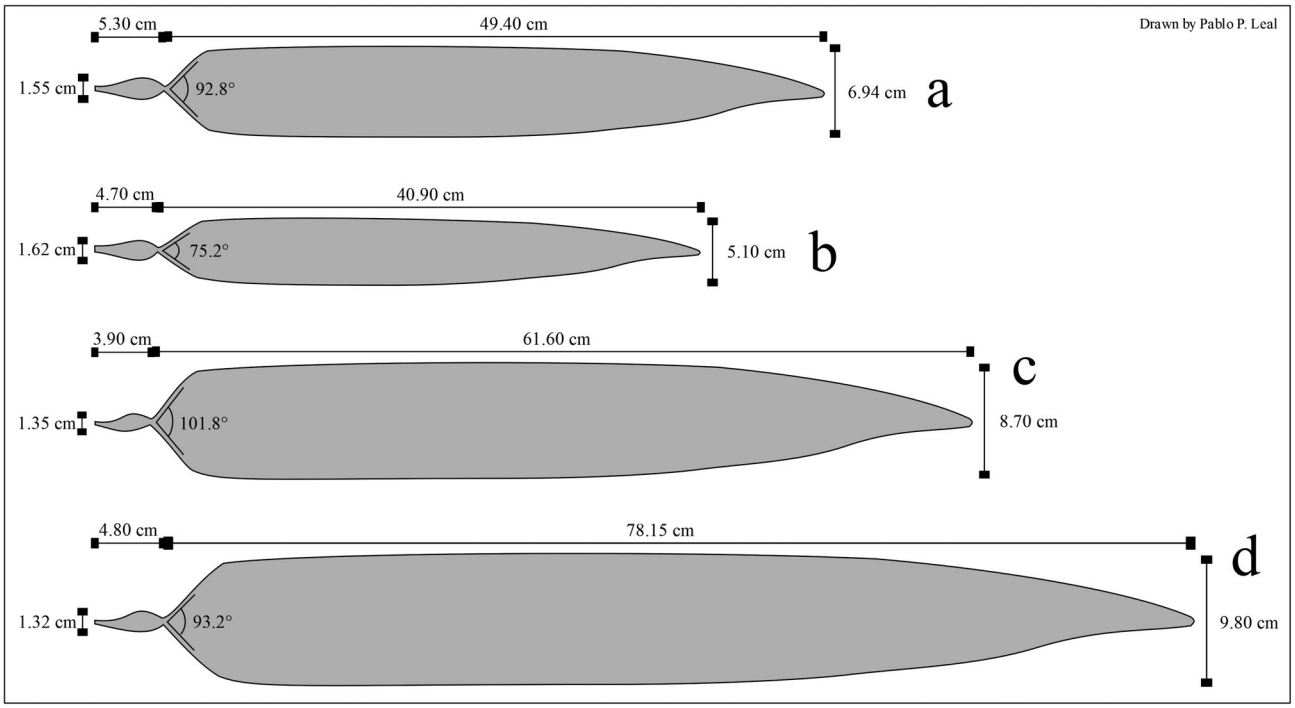

FIG. 12. Average variations in dimensions of vegetative pneumatocyst-bearing blades of *Macrocystis pyrifera* sporophytes from (a) Butterfly Bay, (b) Shag Point, (c) Hamilton Bay, and (d) Macandrew Bay. See text for details.

Santelices et al. 1995) in crevices, under rocks, under the canopy of other seaweeds that may survive during periods of low irradiance and low temperatures such as winter conditions to recover the population in spring (Ladah et al. 1999, Buschmann et al. 2004, Mohring et al. 2013, Schoenrock et al. 2021). For example, Kinlan et al. (2003) proposed that microscopic sporophytes of *M. pyrifera* from California might be a source of delayed recruitment in natural forests because they tolerate low light conditions for 1 month in laboratory experiments. Furthermore, gametophytes and/or microscopic sporophytes of the kelps *Alaria marginata* and *Nereocystis luetkeana* were found, using molecular tools, long after (>1 month) meiospore release, suggesting the existence of seed banks of these kelps in California (Schoenrock et al. 2021). Understanding the developmental processes of early life stages of *M. pyrifera* and the formation of seed banks might help to answer why this kelp species has perennial and annual biological patterns in environments with different exposure to wave action (Buschmann et al. 2004, Schoenrock et al. 2021).

Macroalgae have been categorized as seasonal responders or anticipators (Kain 1989) or Type I and II responders (Lüning and tom Dieck 1989), depending on annual patterns of growth and reproduction. Seasonal responders grow and reproduce when environmental conditions are favorable without clearly defined periods, while seasonal anticipators grow and reproduce according to endogenous regulation and not as a response to suitable environmental conditions (Kain 1989). *Macrocystis pyrifera* is thought to be a season responder (Kain 1989) because its growth rate is directly influenced by variations in nitrogen concentrations (<0.5– ~18 μM) through the year in southern California (North and Zimmerman 1984, Zimmerman and Kremer 1984). Similarly, *M. pyrifera* from Portobello, Otago Harbour was categorized as a seasonal responder because local environmental conditions (i.e., irradiance and nutrients) are adequate to support a constant growth throughout the year (Brown et al. 1997). Although growth was not measured here, we found continuous abundance and reproduction of this kelp and nitrogen availability in the seawater throughout the year, also supporting the idea that *M. pyrifera* from southern New Zealand is a seasonal responder. However, the necessary experiments to verify that *M. pyrifera* is a responder species have not been performed (Agrawal 2012). To date, the study of factors that control sporogenesis have been mainly studied for anticipator species such as *Laminaria* spp. and *Saccharina* spp. (Bartsch et al. 2008), where daylength (i.e., photoperiod) is considered the main abiotic factor that controls reproduction (Wiencke et al. 2009).

We observed that *Macrocystis pyrifera* from south-eastern New Zealand exhibited morphological variation related to wave-exposure similar to previous reports for kelps (Koehl 1986, Hurd 2000,

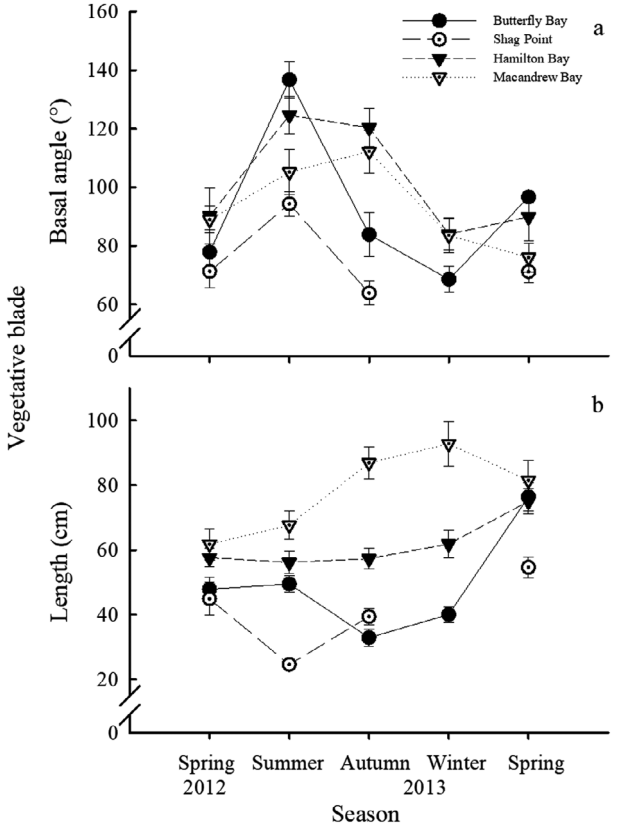

FIG. 13. Annual variation in the (a) basal angle and (b) length of vegetative blades of *Macrocystis pyrifera* from the four study sites (Butterfly Bay, Shag Point, Hamilton Bay, Macandrew Bay). Circles and triangle indicate wave exposure (wave-exposed and wave-protected, respectively) and mean ± SE ($n = 10$). Tukey HSD ($P < 0.05$) showed statistical differences for the basal angle between sites and season, and for length of vegetative blades, sites and season. Note the break and different scales in the *y*-axes.

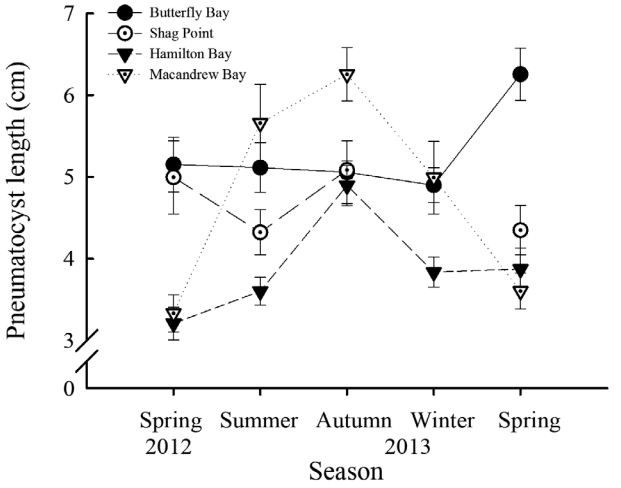

FIG. 14. Annual variation in the length of pneumatocysts of *Macrocystis pyrifera* from the four study sites (Butterfly Bay, Shag Point, Hamilton Bay, Macandrew Bay). Circles and triangle indicate wave exposure (wave-exposed and wave-protected, respectively) and mean ± SE ($n = 10$). Tukey HSD ($P < 0.05$) showed statistical differences for the length of pneumatocysts between sites. Note the break and different scales in the *y*-axes.

Fowler-Walker et al. 2006, Koehl et al. 2008, Coppin et al. 2020). These differences in morphology are attributed to the influence of local environmental conditions (e.g., hydrodynamic forces that differ with wave-exposure) on the phenotypic plasticity of kelps (Hurd 2000, Koehl et al. 2008, Camus et al. 2018). For example, bigger vegetative blades (basal angle, width, and length) in individuals from wave-protected sites increase the surface area for light harvesting, nutrients, and gas exchange in slow water motion conditions while narrow vegetative blades in wave-exposed areas reduce drag forces under rapid flow conditions (Cheshire and Hallam 1988, Blanchette 1997, Hurd et al. 1997, Andrew and Viejo 1998, Koehl et al. 2008). Another noticeable morphological difference between individuals from wave-protected and wave-exposed sites was the holdfast dimension. This may be related to the depth and substratum to which *M. pyrifera* is attached. For example, Demes et al. (2009) indicated that the height of the holdfast increase from the intertidal to the subtidal at a single study site. At sites inside Otago Harbour, the substrate is a mixture of loose rocks and shells on coarse sand (Paavo and Probert 2008) while, in the wave-exposed sites, the substrate is rocky boulders on bedrock (P. Leal pers. obs.). Thus, holdfasts in the wave-protected sites are wider to enable attachment to an unstable substrate than holdfasts from wave-exposed sites that can firmly attach to stable boulders and bedrocks (P. P. Leal, pers. obs.). Both cases indicate that holdfast morphology in *M. pyrifera* can vary through plasticity as a strategy to survive in local conditions of water turbulence and substrate landscape (North 1987, Demes et al. 2009, Camus et al. 2018).

In conclusion, sporogenesis in *Macrocystis pyrifera* from Southern New Zealand was not different between wave-exposure conditions and observed all year round in three of the four study sites, with the exception being the wave-exposed Shag Point in winter. In contrast, sporophyte morphology varied between sites with different wave exposure. Seasonal occurrence and physiological regulation of sporogenesis in sporophyllous and non-sporophyllous laminae and reproductive effort in *M. pyrifera* are still not well understood. We hypothesize that the energetic costs associated with reproduction and growth throughout the year are satisfied by constant favourable conditions of abiotic factors such as nutrients, light, and temperature. Moreover, sporogenesis on blades and apical scimitars in addition to sporophylls requires more investigation to describe its role in short and/or long-distance dispersal of *M. pyrifera*. The fundamental knowledge of the reproductive biology of *M. pyrifera* provides a baseline from which to measure how both climate change

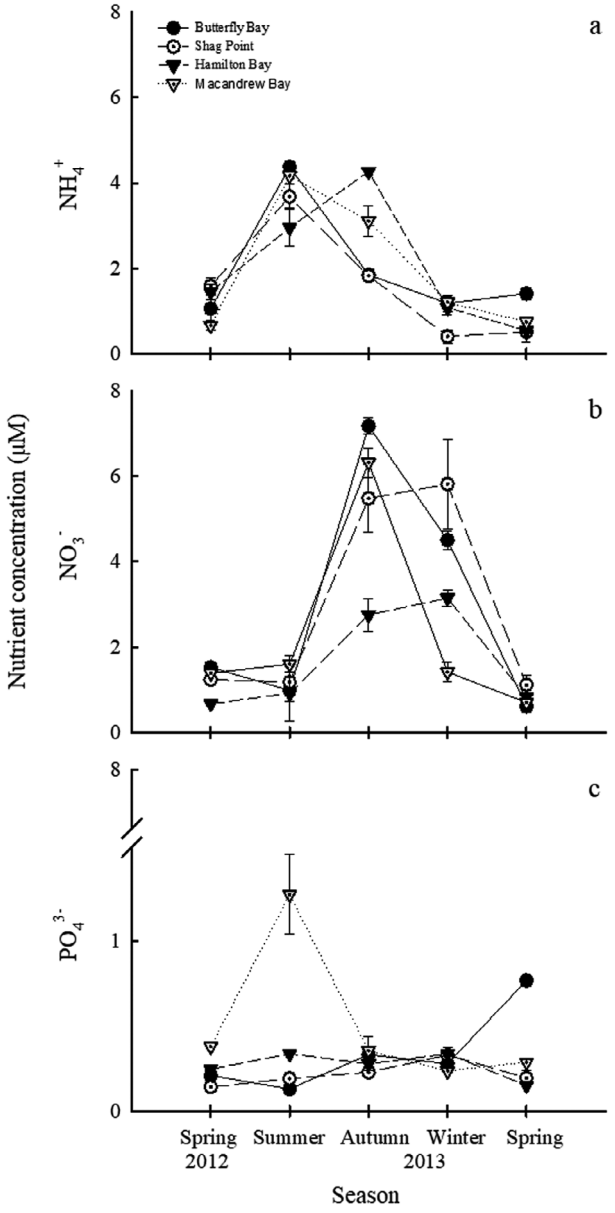

FIG. 15. Annual variation in seawater (a) NH_4^+, (b) NO_3^-, and (c) PO_4^{3-} concentrations in the four study sites (Butterfly Bay, Shag Point, Hamilton Bay, Macandrew Bay). Circles and triangle indicate wave exposure (wave-exposed and wave-protected, respectively) and mean ± SE ($n = 3$). Tukey HSD ($P < 0.05$) showed statistical differences for NH_4^+ between seasons, for NO_3^- between sites and seasons, and for PO_4^{3-} between seasons. Note the break and different scales in the *y*-axes.

(e.g., ocean warming and acidification) will affect reproductive phenology, meiospore viability and, thereby, the resistance of natural kelp populations (Hollarsmith et al. 2020).

ACKNOWLEDGEMENTS

Pablo P. Leal was supported by a scholarship from BECAS CHILE-ANID and by Programa Integral de Desarrollo de Acuicultura de Algas para Pescadores Artesanales (Etapa 4), funded by the Subsecretaría de Economía y Empresas de Menor Tamaño (Convenio 2016). Michael Y. Roleda acknowledges the Philippine's Department of Science and Technology (DOST) Balik Scientist Program for the fellowship. Udo Nitschke gratefully acknowledges support by Skidmore College, 815 North Broadway, Saratoga Springs, NY 12866, USA. Pamela A. Fernández was supported by the Chilean National Commission for Scientific and Technological Research (ANID/FONDECYT; Postdoctoral grant 3170225 and grant 1180647) and ANID/Programa Basal (CeBiB, FB-0001). We are grateful to Rocio Suárez for assisting in field sampling.

AUTHOR CONTRIBUTIONS

P.P. Leal: Conceptualization (equal); data curation (lead); formal analysis (equal); investigation (equal); writing-original draft (lead); writing-review & editing (equal). **M.Y. Roleda**: Conceptualization (equal); writing-review & editing (equal). **P.A. Fernández**: Data curation (equal); investigation (equal); writing-review & editing (equal). **U. Nitschke**: Data curation (equal); formal analysis (equal); writing-review & editing (equal). **C.L. Hurd**: Conceptualization (equal); writing-review & editing (equal).

Agrawal, S. C. 2012. Factors controlling induction of reproduction in algae—review: the text. *Folia Microbiol. (Praha)* 57:387–407.

Akita, S., Yamada, H., Ito, M., Graham, M. H. & Fujita, D. 2016. Sorus formation on the holdfast haptera of the kelp *Ecklonia radicosa* (Phaeophyceae, Laminariales). *Bot. Mar.* 59:433–8.

Andrew, N. L. & Viejo, R. M. 1998. Effects of wave exposure and intraspecific density on the growth and survivorship of *Sargassum muticum* (Sargassaceae: Phaeophyta). *Eur. J. Phycol.* 33:251–8.

Barrales, H. L. & Lobban, C. S. 1975. The comparative ecology of *Macrocystis pyrifera*, with emphasis on the forests of Chubut, Argentina. *J. Ecol.* 63:657–77.

Bartsch, I., Vogt, J., Pehlke, C. & Hanelt, D. 2013. Prevailing sea surface temperatures inhibit summer reproduction of the kelp *Laminaria digitata* at Helgoland (North Sea). *J. Phycol.* 49:1061–73.

Bartsch, I., Wiencke, C., Bischof, K., Buchholz, C. M., Buck, B. H., Eggert, A., Feuerpfeil, P. et al. 2008. The genus *Laminaria sensu lato*: recent insights and developments. *Eur. J. Phycol.* 43:1–86.

de Bettignies, T., Wernberg, T. & Lavery, P. S. 2013. Size, not morphology, determines hydrodynamic performance of a kelp during peak flow. *Mar. Biol.* 160:843–51.

Blanchette, C. A. 1997. Size and survival of intertidal plants in response to wave action: a case study with *Fucus gardneri*. *Ecology* 78:1563–78.

Blanchette, C. A., Miner, B. G. & Gaines, S. D. 2002. Geographic variability in form, size and survival of *Egreria menziesii* around Point Conception, California. *Mar. Ecol. Prog. Ser.* 239:69–82.

Brandt, R. P. 1923. *Potash from Kelp: Early Development and Growth of the Giant Kelp, Macrocystis pyrifera*. U. S. Dept. Agric. Bull. 1191. 40 pp.

Brostoff, W. N. 1988. Taxonomic studies of *Macrocystis pyrifera* (L.) C. Agardh (Phaeophyta) in southern California: holdfasts and basal stipes. *Aquat. Bot.* 31:289–305.

Brown, M. T., Nyman, M. A., Keogh, J. A. & Chin, N. K. M. 1997. Seasonal growth of the giant kelp *Macrocystis pyrifera* in New Zealand. *Mar. Biol.* 129:417–24.

Buschmann, A. H., Moreno, C., Vásquez, J. A. & Hernández-González, M. C. 2006. Reproduction strategies of *Macrocystis*

pyrifera (Phaeophyta) in Southern Chile: the importance of population dynamics. *J. Appl. Phycol.* 18:575–82.

Buschmann, A. H., Vásquez, J. A., Osorio, P., Reyes, E., Filún, L., Hernández-González, M. C. & Vega, A. 2004. The effect of water movement, temperature and salinity on abundance and reproductive patterns of *Macrocystis* spp. (Phaeophyta) at different latitudes in Chile. *Mar. Biol.* 145:849–62.

Camus, C., Faugeron, S. & Buschmann, A. H. 2018. Assessment of genetic and phenotypic diversity of the giant kelp, *Macrocystis pyrifera*, to support breeding programs. *Algal Res.* 30:101–12.

Camus, C., del Hernández-González, M. C. & Buschmann, A. H. 2019. The seaweed resources of Chile over the period 2006–2016: moving from gatherers to cultivators. *Bot. Mar.* 62:237–47.

Chapman, A. R. O. 1987. Population and community ecology of seaweeds. *Adv. Mar. Biol.* 23:1–161.

Cheshire, A. & Hallam, N. D. 1988. Morphology of the southern bull-kelp (*Durvillaea potatorum*, Durvilleales, Phaeophyta) from King Island (Bass Strait, Australia). *Bot. Mar.* 31:139–48.

Chin, N. K. M., Brown, M. T. & Heads, M. J. 1991. The biogeography of Lessoniaceae, with special reference to *Macrocystis* C. Agardh (Phaeophyta: Laminariales). *Hydrobiologia* 215:1–11.

Coppin, R., Rautenbach, C., Ponton, T. J. & Smit, A. J. 2020. Investigating waves and temperature as drivers of kelp morphology. *Front. Mar. Sci.* 7:567.

Dayton, P. K. 1985. Ecology of kelp communities. *Annu. Rev. Ecol. Syst.* 16:215–45.

Demes, K. W., Graham, M. H. & Suskiewicz, T. S. 2009. Phenotypic plasticity reconciles incongruous molecular and morphological taxonomies: the giant kelp, *Macrocystis* (Laminariales, Phaeophyceae), is a monospecific genus. *J. Phycol.* 45:1266–9.

Fernández, P. A., Hurd, C. L. & Roleda, M. Y. 2014. Bicarbonate uptake via anion exchange protein is the main mechanism of inorganic carbon acquisition by the giant kelp *Macrocystis pyrifera* (Laminariales, Phaeophyceae) under variable pH. *J. Phycol.* 50:998–1008.

Fernández, P. A., Roleda, M. Y. & Hurd, C. L. 2015. Effects of ocean acidification on the photosynthetic performance, carbonic anhydrase activity and growth of the giant kelp *Macrocystis pyrifera*. *Photosynth. Res.* 124:293–304.

Fernández, P. A., Roleda, M. Y., Leal, P. P. & Hurd, C. L. 2016. Seawater pH, and not inorganic nitrogen source, affects pH at the blade surface of *Macrocystis pyrifera*: implications for responses of the giant kelp to future oceanic conditions. *Physiol. Plant.* 159:107–19.

Fernández, P. A., Roleda, M. Y., Leal, P. P., Hepburn, C. D. & Hurd, C. L. 2017. Tissue nitrogen status does not alter the physiological responses of *Macrocystis pyrifera* to ocean acidification. *Mar. Biol.* 164:177.

Filbee-Dexter, K. & Wernberg, T. 2018. Rise of turfs: a new battlefront for globally declining kelp forests. *Bioscience* 68:64–76.

Flores-Moya, A. 2012. Warm temperate seaweed communities: a case study of deep water kelp forests from the Alboran Sea (SW Mediterranean Sea) and the Strait of Gibraltar. *In* Wiencke, C. & Bischof, K. [Eds.] *Seaweed Biology*. Springer-Verlag, Berlin Heidelberg, pp 471–93.

Fowler-Walker, M. J., Wernberg, T. & Connell, S. D. 2006. Differences in kelp morphology between wave sheltered and exposed localities: morphologically plastic or fixed traits? *Mar. Biol.* 148:755–67.

Gerard, V. A. & Mann, K. H. 1979. Growth and production of *Laminaria longicruris* (Phaeophyta) population exposed to different intensities of water movement. *J. Phycol.* 15:33–41.

GPS Nautical Charts 2020. *Otago Harbour-Upper Harbour, NU (Marine Chart: NZ_NZ6612_2).*

Graham, M. H. 2002. Prolonged reproductive consequences of short-term biomass loss in seaweeds. *Mar. Biol.* 140:901–11.

Graham, M. H., Kinlan, B. P., Druehl, L. D., Garske, L. E. & Banks, S. 2007a. Deep-water kelp refugia as potential hotspots of tropical marine diversity and productivity. *Proc. Natl. Acad. Sci. USA* 104:16576–80.

Graham, M. H., Vásquez, J. A. & Buschmann, A. H. 2007b. Global ecology of the giant kelp *Macrocystis*: from ecotypes to ecosystems. *Oceanogr. Mar. Biol. An Annu. Rev.* 45:39–88.

Hay, C. H. 1990. The distribution of *Macrocystis* (Phaeophyta: Laminariales) as a biological indicator of cool sea surface temperature, with special reference to New Zealand waters. *J. R. Soc. New Zeal.* 20:313–36.

Hodgson, W. A. 1966. Coastal processes around the Otago Peninsula. *New Zeal. J. Geol. Geophys.* 9:76–90.

Hoffmann, A. J. & Santelices, B. 1997. *Marine Flora of Central Chile*. Ediciones Universidad Católica de Chile, Santiago, Chile, 434 pp.

Hollarsmith, J. A., Buschmann, A. H., Camus, C. & Grosholz, E. D. 2020. Varying reproductive success under ocean warming and acidification across giant kelp (*Macrocystis pyrifera*) populations. *J. Exp. Mar. Bio. Ecol.* 522:151247.

Hurd, C. L. 2000. Water motion, marine macroalgal physiology, and production. *J. Phycol.* 36:453–72.

Hurd, C. L., Harrison, P. J. & Druehl, L. D. 1996. Effect of seawater velocity on inorganic nitrogen uptake by morphologically distinct forms of *Macrocystis integrifolia* from wave-sheltered and exposed sites. *Mar. Biol.* 126:205–14.

Hurd, C. L. & Pilditch, C. A. 2011. Flow-induced morphological variations affect diffusion boundary-layer thickness of *Macrocystis pyrifera* (Heterokontophyta, Laminariales). *J. Phycol.* 47:341–51.

Hurd, C. L., Stevens, C. L., Laval, B. E., Lawrence, G. A. & Harrison, P. J. 1997. Visualization of seawater flow around morphologically distinct forms of the giant kelp *Macrocystis integrifolia* from wave-sheltered and exposed sites. *Limnol. Oceanogr.* 42:156–63.

Jayathilake, D. R. M. & Costello, M. J. 2020. A modelled global distribution of the kelp biome. *Biol. Conserv.* 252:108815.

Jayathilake, D. R. M. & Costello, M. J. 2021. Version 2 of the world map of laminarian kelp benefits from more Arctic data and makes it the largest marine biome. *Biol. Conserv.* 257:109099.

Johnson, C. R., Banks, S. C., Barrett, N. S., Cazassus, F., Dunstan, P. K., Edgar, G. J., Frusher, S. D. et al. 2011. Climate change cascades: shifts in oceanography, species' ranges and subtidal marine community dynamics in eastern Tasmania. *J. Exp. Mar. Bio. Ecol.* 400:17–32.

Kain, J. M. 1982. Morphology and growth of the giant kelp *Macrocystis pyrifera* in New Zealand and California. *Mar. Biol.* 67:143–57.

Kain, J. M. 1989. The seasons in the subtidal. *Br. Phycol. J.* 24:203–15.

Kawai, H., Hanyuda, T., Ridgway, L. M. & Holser, K. 2013. Ancestral reproductive structure in basal kelp *Aureophycus aleuticus*. *Sci. Rep.* 3:2491.

Kim, J. K., Stekoll, M. S. & Yarish, C. 2019. Opportunities, challenges and future directions of open water seaweed aquaculture in the USA. *Phycologia* 58:446–61.

Kinlan, B. P., Graham, M. H., Sala, E. & Dayton, P. K. 2003. Arrested development of giant kelp (*Macrocystis pyrifera*, Phaeophyceae) embryonic sporophytes: a mechanism for delayed recruitment in perennial kelps? *J. Phycol.* 57:47–57.

Koehl, M. A. R. 1986. Seaweeds in moving water: form and mechanical function. *In* Givnish, T. J. [Ed.] *On the Economy of Plant Form and Function*. First. New York: Cambridge University Press. pp 603–34.

Koehl, M. A. R. & Alberte, R. S. 1988. Flow, flapping, and photosynthesis of *Nereocystis luetkeana*: a functional comparison of undulate and flat blade morphologies. *Mar. Biol.* 99:435–44.

Koehl, M. A. R., Silk, W. K., Liang, H. & Mahadevan, L. 2008. How kelp produce blade shapes suited to different flow regimes: a new wrinkle. *Integr. Comp. Biol.* 48:834–51.

Krumhansl, K. A., Okamoto, D. K., Rassweiler, A., Novak, M., Bolton, J. J., Cavanaugh, K. C., Connell, S. D. et al. 2016. Global patterns of kelp forest change over the past half-century. *Proc. Natl. Acad. Sci. USA* 113:13785–90.

Ladah, L. B., Zertuche-González, J. A. & Hernández-Carmona, G. 1999. Giant kelp (*Macrocystis pyrifera*, Phaeophyceae) recruitment near its southern limit in Baja California after mass disappearance during ENSO. *J. Phycol.* 1112:1106–12.

Leal, P. P., Hurd, C. L. & Roleda, M. Y. 2014. Meiospores produced in sori of non-sporophyllous laminae of *Macrocystis pyrifera* (Laminariales, Phaephyceae) may enhance reproductive output. *J. Phycol.* 50:400–5.

Leal, P. P., Hurd, C. L., Sander, S. G., Kortner, B. & Roleda, M. Y. 2016. Exposure to chronic and high dissolved copper concentrations impede meiospore development of the kelps *Macrocystis pyrifera* and *Undaria pinnatifida* (Ochrophyta). *Phycologia* 55:12–20.

Leal, P. P., Hurd, C. L., Fernández, P. A. & Roleda, M. Y. 2017a. Meiospore development of the kelps *Macrocystis pyrifera* and *Undaria pinnatifida* under ocean acidification and ocean warming: independent effects are more important than their interaction. *Mar. Biol.* 164:7.

Leal, P. P., Hurd, C. L., Fernández, P. A. & Roleda, M. Y. 2017b. Ocean acidification and kelp development: reduced pH has no negative effects on meiospore germination and gametophyte development of *Macrocystis pyrifera* and *Undaria pinnatifida*. *J. Phycol.* 53:557–66.

Leal, P. P. & Roleda, M. Y. 2018. Heavy metal ecotoxicity on the early life history stages of macroalgae. *In* Charrier, B., Wichard, T. & Reddy, C. R. K. [Eds.] *Protocols for Macroalgae Research*. CRC Press, Florida, pp 115–27.

Levyns, M. R. 1933. Sexual reproduction in *Macrocystis pyrifera* Ag. *Ann. Bot.* XLVII:349–53.

Liu, X., Bogaert, K., Engelen, A. H., Leliaert, F., Roleda, M. Y. & De Clerck, O. 2017. Seaweed reproductive biology: environmental and genetic controls. *Bot. Mar.* 60:98–108.

Lobban, C. S. 1978. The growth and death of the *Macrocystis* sporophyte (Phaeophyceae, Laminariales). *Phycologia* 17:196–212.

Lüning, K. & tom Dieck, I. 1989. Environmental triggers in algal seasonality. *Bot. Mar.* 32:389–98.

Mann, K. H. 1973. Seaweeds: their productivity and strategy for growth. *Science* 182:975–81.

Mckee, J. W. A., Kavalieris, L., Brasch, D. J., Brown, M. T. & Melton, L. D. 1992. Alginate content and composition of *Macrocystis pyrifera* from New Zealand. *J. Appl. Phycol.* 4:357–69.

Miller, R. J., Lafferty, K. D., Lamy, T., Kui, L., Rassweiler, A. & Reed, D. C. 2018. Giant kelp, *Macrocystis pyrifera*, increases faunal diversity through physical engineering. *Proceedings. Biol. Sci. B.* 285:20172571.

Mohring, M. B., Wernberg, T., Kendrick, G. A. & Rule, M. J. 2013. Reproductive synchrony in a habitat-forming kelp and its relationship with environmental conditions. *Mar. Biol.* 160:119–26.

Moore, L. B. 1942. Observations on the growth of *Macrocystis* in New Zealand. With a description of a free-living form. *Trans. R. Soc. New Zeal.* 72:333–40.

Mora-Soto, A., Palacios, M., Macaya, E., Gómez, I., Huovinen, P., Pérez-Matus, A., Young, M., Golding, N., Toro, M., Yaqub, M. & Macias-Fauria, M. 2020. A high-resolution global map of giant kelp (*Macrocystis pyrifera*) forests and intertidal green algae (Ulvophyceae) with sentinel-2 imagery. *Remote Sens.* 12:694.

Neushul, M. 1963. Studies on the giant kelp, *Macrocystis* II. Reproduction. *Am. J. Bot.* 50:354–9.

Neushul, M. & Haxo, F. T. 1963. Studies on the giant kelp, *Macrocystis*. I. Growth of young plants. *Am. J. Bot.* 50:349–53.

North, W. J. 1987. Biology of the *Macrocystis* resource in North America. *In* Doty, M. S., Caddy, J. F. & Santelices, B. [Eds.] *Case Studies of Seven Commercial Seaweeds Resources*. FAO, San Francisco, California, p 311.

North, W. J. & Zimmerman, R. C. 1984. Influences of macronutrients and water temperatures on summertime survival of *Macrocystis* canopies. *Hydrobiologia* 116–117:419–24.

Nyman, M. A., Brown, M. T., Neushul, M. & Keogh, J. A. 1990. *Macrocystis pyrifera* in New Zealand: testing two mathematical models for whole plant growth. *J. Appl. Phycol.* 2:249–57.

Nyman, M. A., Brown, M. T., Neushul, M., Harger, B. W. W. & Keogh, J. A. 1993. Mass distribution in the fronds of *Macrocystis pyrifera* from New Zealand and California. *Hydrobiologia* 260:57–65.

Paavo, B. & Probert, K. 2008. *Benthic Habitat Structures and Macrofauna of Lower Otago Harbour*. Benthic Science Ltd., Dunedin, New Zealand, 60 pp.

Papenfuss, G. F. 1942. Studies of South African Phaeophyceae. I. *Ecklonia maxima*, *Laminaria pallida*, *Macrocystis pyrifera*. *Am. J. Bot.* 29:15–24.

Pickrill, R. A. & Mitchell, J. S. 1979. Ocean wave characteristics around New Zealand. *New Zeal. J. Mar. Freshw. Res.* 13:501–20.

Pirker, J. G. 2002. *Demography, Biomass Production and Effects of Harvesting Giant Kelp Macrocystis pyrifera* (Linnaeus) in Southern New Zealand. University of Canterbury, Christchurch, New Zealand, 229 pp.

Raven, J. A. & Hurd, C. L. 2012. Ecophysiology of photosynthesis in macroalgae. *Photosynth. Res.* 113:105–25.

Reed, D. C. 1987. Factors affecting the production of sporophylls in the giant kelp *Macrocystis pyrifera* (L.) C.Ag. *J. Exp. Mar. Bio. Ecol.* 113:61–9.

Reed, D. C., Ebeling, A. W., Anderson, T. W. & Anghera, M. 1996. Differential reproductive responses to fluctuating resources in two seaweeds with different reproductive strategies. *Ecology* 77:300–16.

Reed, D. C., Rassweiler, A. & Arkema, K. K. 2008. Biomass rather than growth rate determines variation in net primary production by giant kelp. *Ecology* 89:2493–505.

Reed, D. C., Rassweiler, A., Carr, M. H., Cavanaugh, K. C., Daniel, P. & Siegel, D. A. 2011. Wave disturbance overwhelms top-down and bottom-up control of primary production in California kelp forests. *Ecology* 92:2108–16.

Roleda, M. Y. & Dethleff, D. 2011. Storm-generated sediment deposition on rocky shores: simulating burial effects on the physiology and morphology of *Saccharina latissima* sporophytes. *Mar. Biol. Res.* 7:213–23.

Santelices, B., Hoffmann, A. J., Aedo, D., Bobadilla, M. I. & Otaiza, R. 1995. A bank of microscopic forms on disturbed boulders and stones in tide pools. *Mar. Ecol. Prog. Ser.* 129:215–28.

Schiel, D. R. & Foster, M. S. 2006. The population biology of large brown seaweeds: ecological consequences of multiphase life histories in dynamic coastal environments. *Annu. Rev. Ecol. Evol. Syst.* 37:343–72.

Schiel, D. R. & Foster, M. S. 2015. *The Biology and Ecology of Giant Kelp Forests*. University of California Press, Oakland, California, 416 pp.

Schoenrock, K. M., McHugh, T. A. & Krueger-Hadfield, S. A. 2021. Revisiting the 'bank of microscopic forms' in macroalgal-dominated ecosystems. *J. Phycol.* 57:14–29.

Single, M., Bell, R. & Mccomb, P. 2010. *Physical Coastal Environment of Otago Harbour and Offshore: Assessment of Effects of Proposed Dredging by Port Otago Ltd.* Shore Processes and Management Ltd. 75 pp.

Steneck, R. S., Graham, M. H., Bourque, B. J., Corbett, D., Erlandson, J. M., Estes, J. A. & Tegner, M. J. 2002. Kelp forest ecosystems: biodiversity, stability, resilience and future. *Environ. Conserv.* 29:436–59.

Stevens, C. L. & Hurd, C. L. 1997. Boundary-layers around bladed aquatic macrophytes. *Hydrobiologia* 346:119–28.

van Tussenbroek, B. I. 1989. Seasonal growth and composition of fronds of *Macrocystis pyrifera* in the Falkland Islands. *Mar. Biol.* 100:419–30.

Wernberg, T. & Thomsen, M. S. 2005. The effect of wave exposure on the morphology of *Ecklonia radiata*. *Aquat. Bot.* 83:61–70.

Wiencke, C., Gómez, I. & Dunton, K. 2009. Phenology and seasonal physiological performance of polar seaweeds. *Bot. Mar.* 52:585–92.

Wing, S. R., Leichter, J. J., Perrin, C., Rutger, S. M., Bowman, M. H. & Cornelisen, C. D. 2007. Topographic shading and wave exposure influence morphology and ecophysiology of

Ecklonia radiata (C. Agardh 1817) in Fiordland, New Zealand. *Limnol. Oceanogr.* 52:1853–64.

Wing, S. R. & Patterson, M. R. 1993. Effects of wave-induced light-flecks in the intertidal zone on photosynthesis in the macroalgae *Postelsia palmaeformis* and *Hedophyllum sessile* (Phaeophyceae). *Mar. Biol.* 116:519–25.

Womersley, H. B. S. 1987. *The Marine Benthic Flora of Southern Australia. Part II.* South Australian Government Printing Division, Adelaide, Australia, 481 pp.

Zimmerman, R. C. & Kremer, J. N. 1984. Episodic nutrient supply to a kelp forest ecosystem in southern California. *J. Mar. Res.* 42:591–604.

Supporting Information

Additional Supporting Information may be found in the online version of this article at the publisher's web site:

Figure S1. Annual variation in holdfast (b) width of *Macrocystis pyrifera* from the four study sites (Butterfly Bay, Shag Point, Hamilton Bay, MacAndrew Bay). Circles and triangle indicate wave exposure (wave-exposed and wave-protected, respectively) and mean ± SE ($n = 10$). Note the break and different scales in the y-axes.

Figure S2. Annual variation in the width of vegetative blades of *Macrocystis pyrifera* from the four study sites (Butterfly Bay, Shag Point, Hamilton Bay, MacAndrew Bay). Circles and triangle indicate wave exposure (wave-exposed and wave-protected, respectively) and mean ± SE ($n = 10$). Note the break and different scales in the y-axes.

Figure S3. Annual variation in the width of pneumatocysts of *Macrocystis pyrifera* from the four study sites (Butterfly Bay, Shag Point, Hamilton Bay, MacAndrew Bay). Circles and triangle indicate wave exposure (wave-exposed and wave-protected, respectively) and mean ± SE ($n = 10$). Note the break and different scales in the y-axes.

Table S1. Sites and dates of seasonal sampling of *Macrocystis pyrifera* populations. In addition, it is indicated when populations of *M. pyrifera* population were found (f.) or not found (n.f.) and when the respective variable was measured (m.) or not measured (n.m.).

Table S2. Total of laminae (and number of sampled sporophylls between square brackets) of each type of fertile lamina (i.e., sporophyll, blades, scimitar) of *Macrocystis pyrifera* from the four study sites used to prepare Figures 4–6. It is also indicated when fertile laminae were not found (n.f.).

Table S3. Statistical summary of univariate linear regressions to determine effects and interactions for each of explanatory variables (Site, Season, Year) on each of the different response variables. Exposure excluded as outlined in the main text. Most response variables were log-transformed in order to better meet test assumptions. Only the Site × Season interaction term was included in models; other interaction terms did not yield meaningful information. Type III sum of squares (SS) were calculated. Tukey HSD tests were applied for multiple pairwise comparisons; group differences are indicated by lowercase letters ($a > b > c > d$). Significant effects were quantified by means of $p\eta^2$. Vegetative Blade Width and Holdfast Width were not analysed due to high collinearity with Vegetative Blade Length and Holdfast Length, respectively.

Table S4. Statistical summary of univariate linear regressions to determine effects and interactions for each of explanatory variables (Site, Season, Year) on each of the different response variables. Exposure excluded as outlined in the main text. Responses were measured on sporophyll from the same sporophyte; medians were calculated from these repeated measures and were considered replicates. Medians of response variables were arcsine-transformed in order to better meet test assumptions. Only the Site × Season interaction term was included in models; other interaction terms did not yield meaningful information. Type III sum of squares (SS) were calculated. Tukey HSD tests were applied for multiple pairwise comparisons; group differences are indicated by lowercase letters ($a > b > c$). Significant effects were quantified by means of $p\eta^2$. Ripeness Stage II (pre-mature) was not analysed due a large fraction of zeros (75% of all observations).

Table S5. Statistical summary of univariate linear regressions to determine effects and interactions for each of explanatory variables (Site, Season, Year) on each of the different response variables. Exposure excluded as outlined in the main text. Response variables were arcsine-transformed in order to better meet test assumptions. Only the Site × Season interaction term was included in models; other interaction terms did not yield meaningful information. Type III sum of squares (SS) were calculated. Tukey HSD tests were applied for multiple pairwise comparisons; group differences are indicated by lowercase letters ($a > b$). Significant effects were quantified by means of $p\eta^2$. Stage II (pre-mature) was not analysed due a large fraction of zeros (73% of all observations).

Table S6. Statistical summary of univariate linear regressions to determine effects and interactions for each of explanatory variables (Site, Season, Year) on each of the different response variables. Exposure excluded as outlined in the main text. Response variables were arcsine-transformed in order to better meet test assumptions.

Only the Site × Season" interaction term was included in models; other interaction terms did not yield meaningful information. Type III sum of squares (SS) were calculated. Tukey HSD tests were applied for multiple pairwise comparisons; group differences are indicated by lowercase letters (a > b). Significant effects were quantified by means of $p\eta^2$. Stage II (pre-mature) was not analyzed due a large fraction of zeros (60% of all observations).

Table S7. Statistical summary of univariate linear regressions to determine effects and interactions for each of explanatory variables (Site, Season, Year) on each of the different response variables. Exposure excluded as outlined in the main text. Responses were measured on sporophylls of individual sporophytes; medians of these repeated measures were considered replicates. Response variables were analysed after reciprocal transformation to better meet test assumptions. Only the Site × Season interaction term was included in models; other interaction terms did not yield meaningful information. Type III sum of squares (SS) were calculated. Tukey HSD tests were applied for multiple pairwise comparisons; group differences are indicated by lowercase letters (a > b > c). Significant effects were quantified by means of $p\eta^2$.

Table S8. Statistical summary of univariate linear regressions to determine effects and interactions for each of explanatory variables (Site, Season, Year) on each of the different response variables. Exposure excluded as outlined in the main text. Responses were measured on sporophylls of individual sporophytes; medians of these repeated measures were considered replicates. Response variables were analysed after arcsine transformation to better meet test assumptions. Only the Site × Season interaction term was included in models; other interaction terms did not yield meaningful information. Type III sum of squares (SS) were calculated. Tukey HSD tests were applied for multiple pairwise comparisons; group differences are indicated by lowercase letters (a > b > c). Significant effects were quantified by means of $p\eta^2$.

Table S9. Statistical summary of univariate linear regressions to determine effects and interactions for each of explanatory variables (Site, Season, Year) on each of the response variables (NH_4^+,NO_3^-,PO_4^{3-}). Exposure excluded as outlined in the main text. Response variables were log-transformed. Only the Site × Season interaction term was included in models; other interaction terms did not yield meaningful information. Type III sum of squares (SS) were calculated. Tukey HSD tests were applied for multiple pairwise comparisons; group differences are indicated by lowercase letters (a > b). Significant effects were quantified by means of partial eta-squared ($p\eta^2$).